Journal of Mining and Environment (JME)

journal homepage: www.jme.shahroodut.ac.ir

Vol. 11, No. 1, 2020, 99-117.
DOI: 10.22044/jme.2019.8465.1727

Identification of Geochemical Anomalies Using Fractal and LOLIMOT Neuro-Fuzzy modeling in Mial Area, Central Iran

M. Alipour Shahsavari[1*], P. Afzal[2], A. Hekmatnejad[3]

1. Department of Mining Engineering, Faculty of Engineering, Tehran University, Tehran, Iran
2. Department of Mining Engineering, South Tehran branch, Islamic Azad University, Tehran, Iran
3. Department of Mining Engineering, Advanced Mining Technology Center, University of Chile, Chile

Received 26 May 2019; received in revised form 1 October 2019; accepted 6 November 2019

Keywords

Concentration-number fractal model

Local linear model tree;

Mial.

Abstract

The Urumieh-Dokhtar Magmatic Arc (UDMA) is recognized as an important porphyry, disseminated, vein-type, and polymetallic mineralization arc. In this work, we aim to identify and subsequently determine the geochemical anomalies for exploration of Pb, Zn, and Cu mineralization in the Mial district situated in UDMA. The factor analysis, Concentration-Number (C-N) fractal model, and Local Linear Model Tree (LOLIMOT) algorithm are used for this purpose. The factor analysis is utilized in recognition of the correlation between the elements and their classification. This classified data is used for training the LOLIMOT algorithm based on the relevant elements. The results of the LOLIMOT algorithm represent anomalies in the areas with no lithogeochemical samples, although the C-N log-log plot for target elements are generated based on the stream sediment and lithogeochemical samples, which can be delineated by the mineral potential maps of the target elements. The results obtained by the LOLIMOT and fractal modeling show that the SW and the Eastern parts of the area are proper for further exploration of Cu, Pb, and Zn.

1. Introduction

The Urumieh-Dokhtar Magmatic Arc (UDMA) was formed as a result of the sub-division of the Zagros orogenies in the Cenozoic era, and it is a thick and linear intrusive-extrusive complex. UDMA comprises several lithological units including small to large plutonic bodies (diorites, granodiorites, gabbro, and granites) and widely distributed basaltic lava flows, trachybasalt (locally shoshonitic), andesite, dacite, trachyte, ignimbrites, and pyroclastic. The youngest rocks are lava flows and pyroclastic from Quaternary and the oldest known pluton in this assemblage cuts across the Upper Jurassic formations and overlain uncomfortably by Lower Cretaceous fossiliferous [1–3].

Geochemical exploration has been used for mineral prospecting in the different types of deposits [4, 5]. The critical challenge is to identify the geochemical anomalies from the background and separation of the highly and extremely geochemical anomalies [6–9]. The stream sediment data plays an important role in the discrimination of different anomalies with the determination of elemental thresholds in the reconnaissance and prospecting stages [10–13].

Without a correct geochemical interpretation of the datasets, defining the anomalies can lead to areas without a mineralization potential. Using the conventional statistical methods such as the histogram analysis, summation of mean, standard deviation, and box plot for defining the anomalies are required to be used cautiously because of the particular characteristics of the geochemical data [7, 14–20]. These characteristics include spatial-dependence of data, range of different processes that influence the element abundances measured,

Corresponding author: Mehrnoosh.ap@gmail.com (M. Alipour Shahsavari).

sampling methods, and level of analytical precision. As a result, no single universally applicable statistical test has been developed for identifying the anomalies [14]. Integrating different identifying methods such as the intelligence ones can rise the degree of confidence in the identification of anomaly zones [8, 21–23].
The modern techniques of artificial intelligence (AI) has been applied in almost all the fields of the human knowledge [24, 25]. Combining different intelligent methods is an ongoing research zone in AI. The aim is to achieve a hybrid approach that benefits from all the available components. Machine learning and AI deal with the difficulties that are hard in formulating the algorithms that are needed to be translated into programs [26]. From another viewpoint, AI tries to find the hidden structures in the data, and in this case, the various classes of learning algorithm such as decision tree, support vector machines, and neural networks can be used [26–28].
The fuzzy sets theory was initiated by Lotfi Zadeh [29]. Fuzzy systems suggest a mathematic calculus to interpret the individual human information of the actual processes, and in this way, it will handle real information with a more or less level of uncertainty. The neuro-fuzzy algorithm is a kind of predictor that is a non-linear modeling and it figures out complicated patterns [25].
Due to the aforementioned subjects, determination of the elemental distribution related to the stream sediment and lithogeochemical data using some intelligent method such as neuro-fuzzy algorithm can be very useful [28, 30]. This method improves the performance in combination with the mentioned methods [27, 31, 32].
Moreover, the structural methods, specifically the fractal/multifractal models, have been used for geochemical exploration in different scales since the 1990s [33–40]. Fractal modeling, introduced by Mandelbrot (1983), is commonly applied in dealing with the elemental concentration. These methods include the concentration-number (C-N) [41, 42] concentration-area (C-A) [33] spectrum-area (S-A) [36], concentration-distance [37], and singularity technique models that can be found in numerous studies [21, 43–45].
In this work, an integrated methodology including factor analysis (FA), fractal Concentration-Number (C-N) model, and local linear model tree (LOLIMOT) was applied to identify the geochemical anomalies associated with Pb-Zn and Cu mineralization based on stream sediment, lithogeochemical, and heavy mineral data in Mial district, Central Iran. The main objective of this work was to identify the geochemical anomalies that could provide vectors to mineral resource exploration.

2. Methods

2.1. Factor analysis

One of the dimension-reduction techniques is Factor analysis (FA), which deals with the compositional data [46–48]. The aim of FA is to explain the variation in a multivariate dataset by as limited factors as possible, and also to detect the hidden multivariate data structure [20, 48–51].

2.2. Concentration–number (C-N) fractal model

The C-N fractal model has been proposed by Hassanpour and Afzal (2013) based on the Number-Size (N-S) model established by Mandelbrot (1983), which relates the frequency distribution of the elemental concentrations based on its number of samples by a power-law relation. In this model, the geochemical data has not been faced pre-treatment and evaluation [38, 41, 53, 54].
A similar set of data that shows a distinct pattern can be distinguished by different straight lines fitted to the values of the results obtained from the geological, geochemical, and mineralogical information [55–58]. Geochemical background and different anomalies are separated by the breakpoints between the straight-line segments in the log-log plots that are related to the threshold values.
On the log-log plot, the optimal threshold for distinguishing the geochemical anomalies from the background is the common concentration value on both linear relationships [4, 37, 42].

2.3. LOLIMOT

One of the widespread non-linear model architectures is the local model networks, also known as the Takagi-Sugeno neuro-fuzzy systems [24], [59–64]. Generally, in order to parameterize the local model, a linear approach is used, and usually, the least squares method is used to estimate the mentioned parameters [25], [65–69]. The intelligent and highly independent systems play a great role in both the industrial and academic settings [67], [70], [59], [65], [66], [71].
LOLIMOT is an incremental tree-construction algorithm that partitions the input space by axis-orthogonal splits; it is carried out by a Matlab code

[66]–68], [71]–73]. The inputs and outputs of LOLIMOT are collected into a spread sheet using Microsoft Excel for the analysis and various visualizations of summaries to enhance the discussions of the results.
The divide and conquer strategy is one of the most significant factors for the accomplishment of LOLIMOT [66], [71], [72], [74], [75]. In the Local Linear Models (LLMs), the network output is calculated as a weighted summation of the outputs of each LLM, where the validity function is explained as the operating point-dependent weighting factors. The basic approach with LLM is to divide the input space into small sub-spaces with fuzzy validity functions, which are typically chosen as normalized Gaussians [26], [65], [70], [76–78]. Any created linear part with its validity function can be defined as a fuzzy neuron. Subsequently, the entire model is a neuro-fuzzy network with one hidden layer and a linear neuron in the output layer that basically computes the weighted summation of locally linear model outputs [65], [72], [79], [80].

LOLIMOT is incremental based on three iterative steps. First, the worst LLM is definite based on the local loss function. This LLM neuron is chosen to be divided. In the next step, all partitions of LLMs on the input space are checked. Finally, the best division for the new neuron is added [66], [68], [75], [81–83]. The first five iterations of the LOLIMOT algorithm for a 2D input space is shown in Figure 1.
The important methodology with LLNFM is to divide the input space into small sub-spaces with fuzzy validity functions. Using the fuzzy validity functions is important, particularly in the conjugation of two different linear models, as it helps the conjugation to be a smooth line instead of a broken one. By the results, any created linear part with its validity function can be called a fuzzy neuron. Consequently, the network structure can be described as a neuro-fuzzy network with one hidden layer and the weighted summation of the outputs of locally linear models by a linear neuron in the output layer can simply be calculated [68], [78], [84], [85].

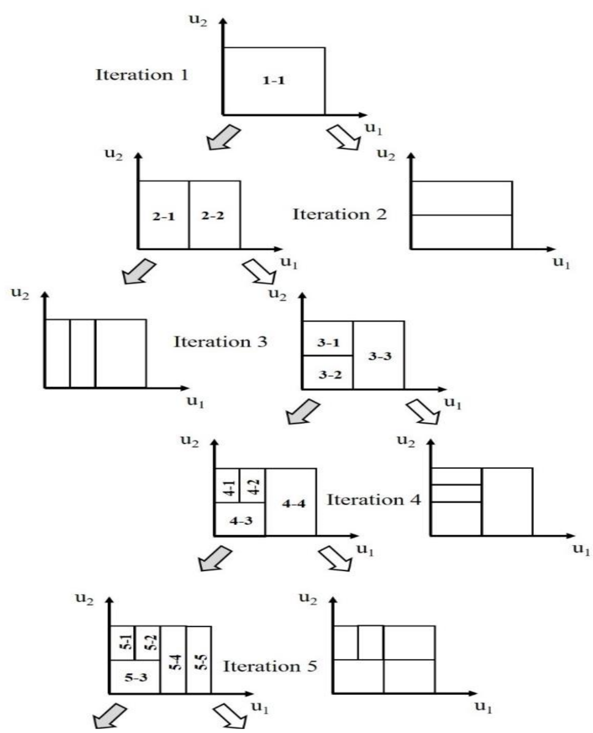

Figure 1. Operation of the LOLIMOT algorithm in the first five iterations for a 2D input space [67].

3. Case Study
3.1. Geological setting
The Mial district is located in the central part of the major magmatic metallogenic belt in Iran, named the Urumieh-Dokhtar magmatic arc (UDMA), which contains copper porphyry deposits with other types of related mineralization such as lead and zinc and epithermal deposits [1], [86]–91]. This prospecting area is shown on the map with the main tectonic units of Iran ([92]; Figure 2).

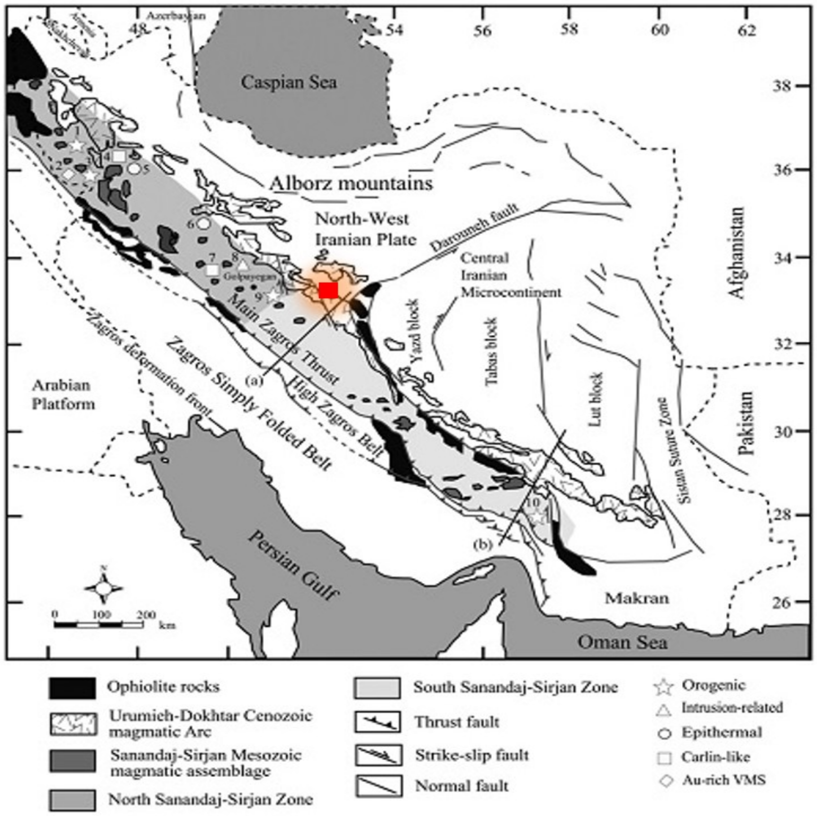

Figure 2. The structural map of Iran [92] with location of the Mial area as a red square.

The central part of UDMA comprises the rock unit from Permian up to Quaternary and intense magmatism activity with Tertiary plutonism [86], [93–96]. The main faults have the NW-SE trend in this region [2]. The geological map of the Mial area with data locations including stream sediment, lithogeochemical data, and heavy mineral is depicted in Figure 3. This area mainly contains lapilli tuff, andesite breccia, red marl, and sandy limestone.

3.2. Dataset

In this work, three types of data were used consisting of the following data (Figure 4):

- 210 stream sediment samples at a density of one sample per 0.1 km^2. Choosing the sample location was based on the stream distributions, which were extracted from the 1:50,000 topographic map and also the number of stream branches. The size of each sample was -80 mesh.
- 98 lithogeochemistry samples were collected from the whole area. These samples were taken using the chip sampling method. The samples were taken from the most potentiated areas and were unsystematic.
- 86 samples were taken from 20 to 30 cm under the stream floor and from the most potentiated areas based on the geochemical expert's opinions for the heavy minerals studied. The sample size was -20 mesh.

The following 12 elements were determined by Inductively Coupled Plasma (ICP) and represented in ppm: Pb, Fe, Al, Ca, Mg, Ag, As, Bi, Co, Cu, Zn and Mo. The remaining element (Au) was determined by fire assay and represented in ppb. The descriptive statistics of the stream sediment and the lithogeochemical data are represented in Table 1.

In order to check the analysis accuracy, 10% of the total samples were divided into two parts with two different codes, and the analysis results were acceptable based on the laboratory standard for repeated samples.

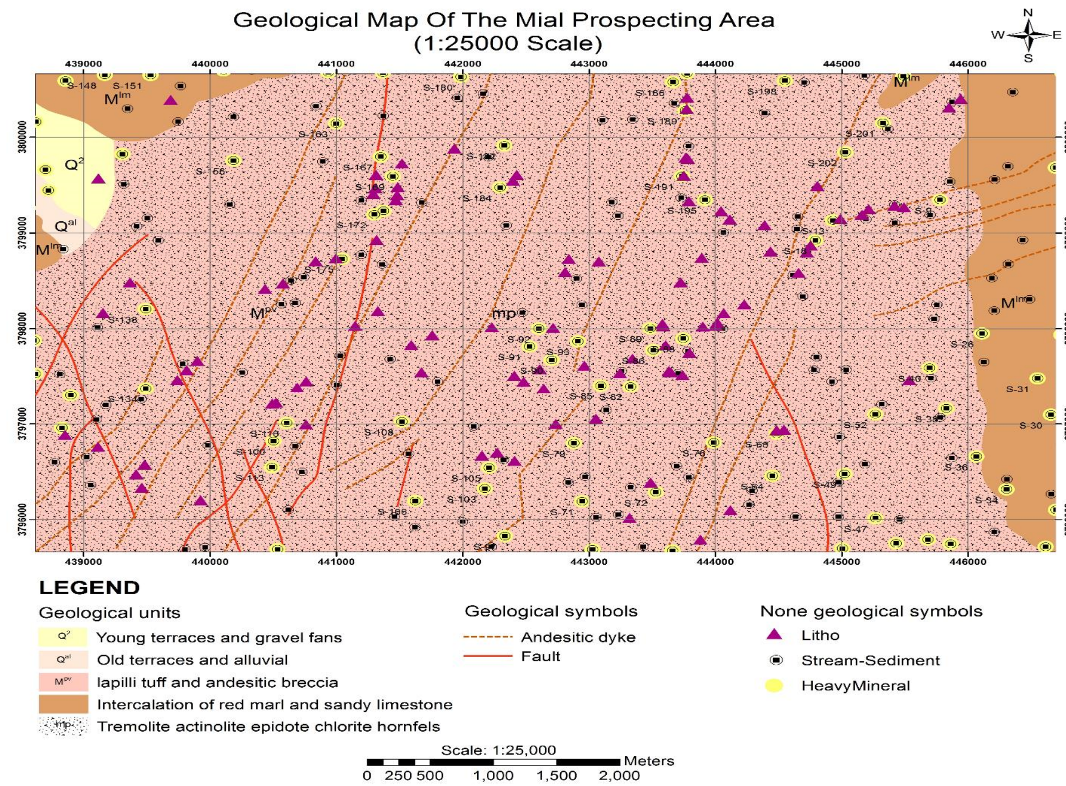

Figure 3. Geological map of the Mial area in scale of 1:25,000.

Table 1. Descriptive statics of lithogeochemistry and stream sediment data.

Elements	N	Minimum	Maximum	Mean	Std. Deviation	Skewness		Kurtosis		Detection Limit (ppm)
	Statistic	Statistic	Statistic	Statistic	Statistic	Statistic	Std. Error	Statistic	Std. Error	
Lithogeochemistry data										
Al	98	7873	98870	77115.13	21154.607	-1.772	.244	2.7	.483	100
Ca	98	2901	236356	52700.28	43335.920	2.282	.244	6.7	.483	100
Fe	98	11638	154182	48949.00	22514.258	2.329	.244	7	.483	100
Mg	98	686	260-03	13017.90	6308.480	-.328	.244	-.5	.483	100
Ag	98	.13	356.50	10.3427	46.33060	6.205	.244	40.8	.483	0.1
As	98	7.1	2726.1	127.399	384.2713	4.866	.244	26.2	.483	0.5
Bi	98	.29	171.30	3.7065	18.17737	8.371	.244	76.3	.483	1
Co	98	7	31	15.52	3.731	1.041	.244	2.4	.483	1
Cu	98	3	33299	797.36	3937.269	6.921	.244	52.0	.483	1
Mo	98	.63	12.86	2.0236	2.07554	2.456	.244	8.0	.483	0.5
Pb	98	10	49798	1717.55	7619.105	5.177	.244	27.3	.483	1
Zn	98	30	1782	169.90	293.981	4.018	.244	17.1	.483	1
Stream sediment data										
Pb	210	7.2	5160.0	128.013	423.3564	8.806	.168	97.3	.334	1
Fe	210	32800	68600	46863.33	6361.234	.462	.168	.7	.334	100
Al	210	56600	101000	79235.24	11033.628	-.183	.168	-.8	.334	100
Ca	210	16400	111000	52440.48	25908.644	.690	.168	-.6	.334	100
Mg	210	11300	28100	17744.29	3057.909	.688	.168	.2	.334	100
Ag	210	.27	5.03	.5701	.52314	6.521	.168	48.1	.334	0.1
As	210	5.2	71.2	18.695	10.6292	2.454	.168	8.0	.334	0.5
Bi	210	.0	1.3	.222	.1461	4.496	.168	26.2	.334	1
Co	210	10.6	26.2	16.673	2.7656	.246	.168	-.2	.334	1
Cu	210	14.1	138.0	36.209	15.3059	2.548	.168	10.9	.334	1
Mo	210	.3	2.5	1.005	.2496	.782	.168	5.6	.334	0.5
Zn	210	69	273	125.10	40.788	1.152	.168	.8	.334	1

4. Discussion

4.1. Classification of data by FA

The stream sediment and geochemical data is required to be pre-processed before FA because of the data closure problem [20, 49, 97]. Using the principal component analysis (PCA) can be helpful in challenge with a large dataset [48, 51, 98–101]. The concentration dataset is divided into subsets, and this is revealed by different factors [102]. The components in each subset are correlated with one another, and are fundamentally independent from the components in the other subsets ([51], Table 2). Here, the factors involved should be representative of the underlying and prior geological and metallogenic process that created the correlations among these variables [57]. Ln transformation is applied to pre-process the data by the PCA method using the SPSS statistical software package in order to find the elemental correlation coefficients.

Table 2. Rotated component matrix for extraction of the factors using PCA.

	Component						
	1	**2**	**3**	**4**	**5**	**6**	**7**
LnCr	-.152	.130	.483	-.107	-.710	-.230	.149
LnMn	.557	-.213	.058	**.644**	.176	-.135	-.111
LnNi	-.044	-.127	.840	-.041	-.292	-.013	-.020
LnPb	.303	.341	-.200	**.723**	.185	.285	.108
LnFe	**.811**	-.003	-.238	.137	-.282	-.077	.020
LnAl	**.867**	.030	-.073	.143	.281	.037	-.207
LnCa	**-.832**	-.242	-.111	-.012	-.259	.061	.004
LnLi	.088	-.163	.426	-.190	-.381	.174	-.567
LnP	.324	.131	.576	.170	.460	-.124	.117
LnMg	**.816**	-.331	-.101	.209	-.061	.115	.008
LnK	-.245	-.078	.819	.163	.209	.125	-.205
LnNa	**.694**	.085	-.178	.099	.259	-.475	-.101
LnZr	.002	-.486	.451	.453	-.130	.325	.168
LnAg	-.046	.248	.014	**.714**	-.180	.234	-.003
LnAs	.152	.817	.038	-.007	.072	-.040	-.188
LnBi	.023	.676	.134	.304	-.081	.118	.239
LnCo	**.942**	.032	-.048	.006	-.105	.015	.075
LnCu	**.742**	.391	.057	.242	.168	.229	.088
LnMo	-.188	.714	.282	.096	-.145	-.322	-.151
LnSb	.434	.461	-.055	.436	.235	.343	.013
LnZn	.239	.073	-.024	**.876**	.171	-.028	-.118
LnCd	.405	.381	.212	.421	.415	-.037	-.122

4.2. Fractal modeling

According to the C-N log-log plots of the stream sediment data, there are four, three, and five geochemical populations for Pb, Zn, and Cu, respectively (Table 3 and Figure 4). These geochemical populations are achieved from the added trendline to the C-N log-log plot, and where there is an abvious change in the data distribution, the trendline will break. Each element (Pb, Zn, and Cu) grade can be divided in to different groups based on these breaks using a simple antilog for 10 to the A power, where A is equal to the number in the x-axis where the break point is located. The grade classification in the corresponding anomaly maps is based on these break points. Moreover, the elemental symbol maps were created by the ArcGIS 10.3.1 software and correlated with geological units, as shown in Figure 4. However, the Pb high-intensity anomalies commence from 977 ppm in the intercalation of red marl, sandy limestone, lapilli tuff, and andesitic breccia rock, which are close to the andesitic dikes and lineament aggregation in the Southern, Eastern, and Western parts of the area (Figure 4). The moderate-intensity Zn anomalies occurred in association with red marl, sandy limestone, lapilli tuff, and andesitic breccia rock, and began from 231 ppm (Figure 4). The moderate-intensity Cu anomal samples have values higher than 95 ppm, which are located in the lapilli tuff and andesitic breccia rock in the Western part of the area (Figure 4).

Regarding the elemental log-log plots for the lithogeochemical data, two geochemical populations for Pb and Zn and three geochemical populations for Cu were distinguished (Table 3 and Figure 5). The lithogeochemical symbol maps were created by the ArcGIS software and correlated with rock types, as depicted in Figure 5. High-intensity anomalies in the lithogeochemical samples for Pb occurred from 25118 ppm. These anomalies are located in lapilli tuff, andesitic breccia, and near lineament aggregation in the SW part of the area (Figure 5). Highly intensive anomalies for Zn (1445 ppm) are spread in the Western part of the Mial area in the lapilli tuff, andesitic breccia, and mostly near one of the biggest andesitic dike and one of the lineaments shown in Figure 6. The high-intensity Cu anomal samples have values higher than 1995 ppm, which are located in the intercalation of red marl, sandy limestone, lapilli tuff, and andesitic breccia in the NW and Southern parts of the area. These anomalies are mostly located near one of the biggest andesitic dikes (Figure 5).

Table 3. Elemental thresholds derived via the C-N model based on the stream sediment samples.

Elements	Low-intensity thresholds	High-intensity thresholds
Pb (ppm)	794	977
Zn (ppm)	208	231
Cu (ppm)	87	95

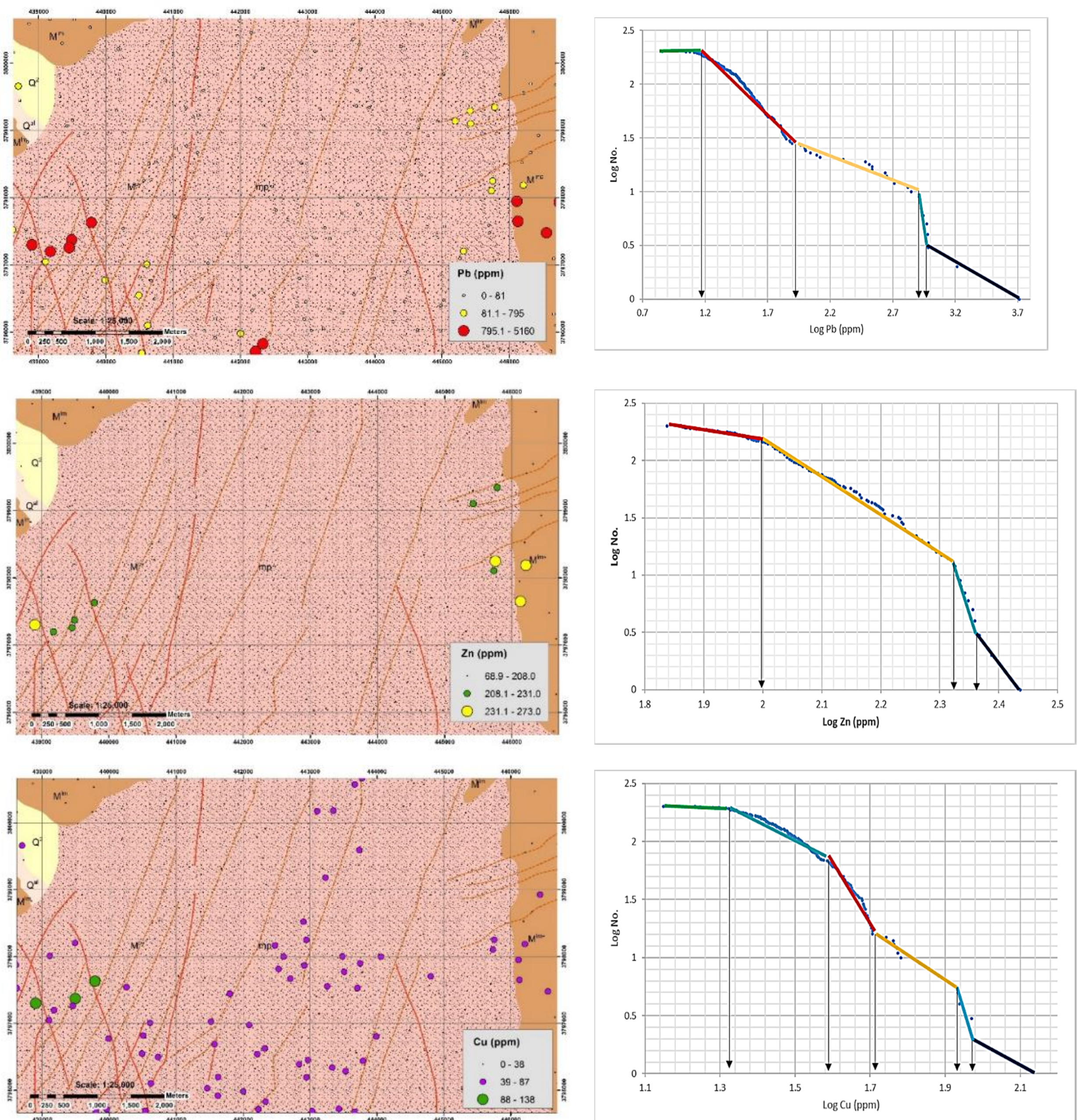

Figure 4. Log-log plots and geochemical anomaly maps resulting from the C-N model for Pb, Zn, and Cu based on the stream sediment samples.

Table 4. C-N elemental thresholds based on the lithogeochemical samples.

Elements	Low-intensity thresholds	High-intensity thresholds
Pb (ppm)	70	25118
Zn (ppm)	45	1445
Cu (ppm)	141	1995

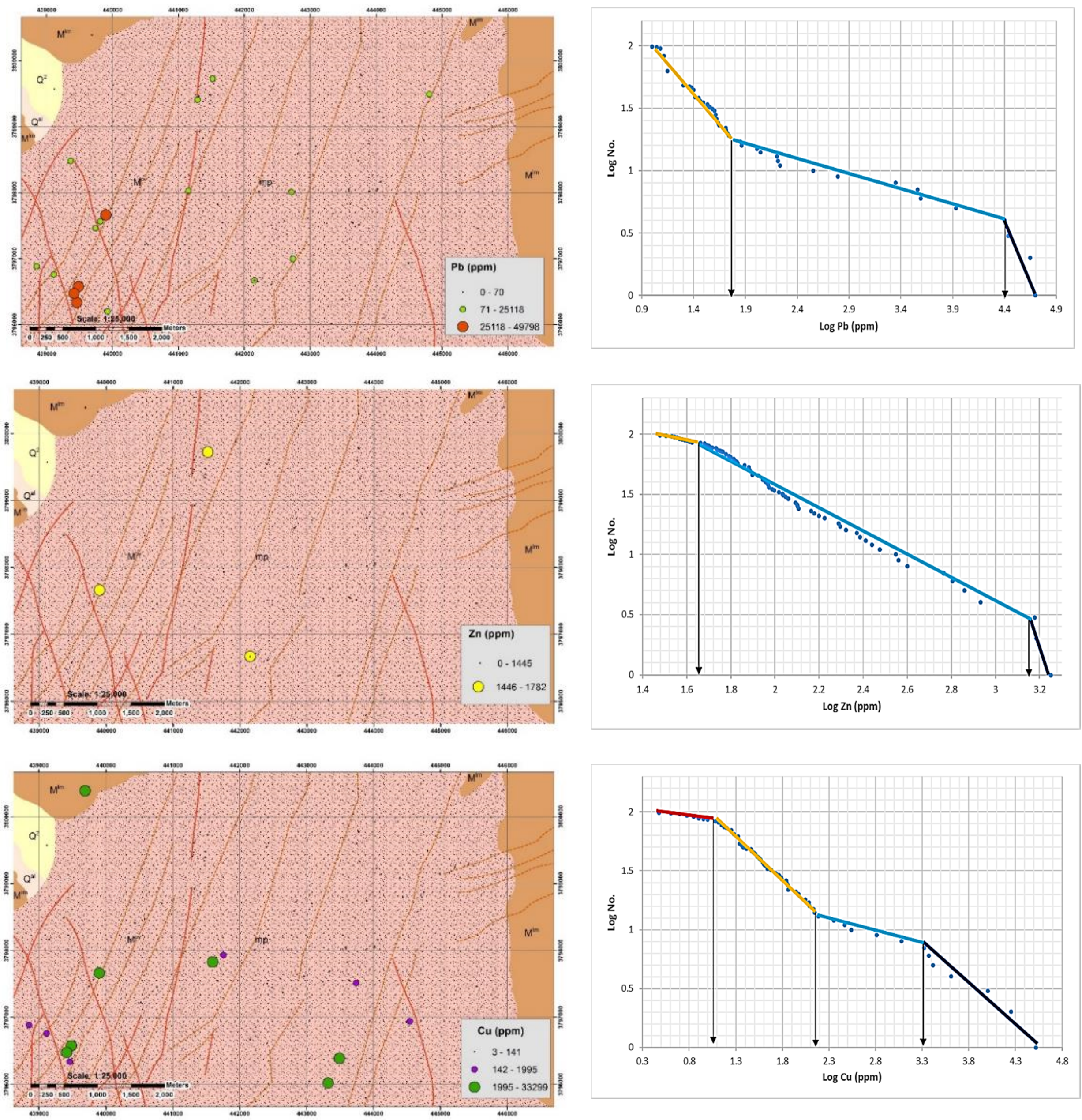

Figure 5. Log-log plots and geochemical anomaly maps resulting from the C-N model for Pb, Zn, and Cu based on the lithogeochemical samples. ***LOLIMOT algorithm***

The stream sediment and lithogeochemical samples were studied to evaluate a neuro-fuzzy method in order to estimate the associated mineralization with Pb, Zn, and Cu. The LLM Tree was applied in the Pb, Zn, and Cu mineralization in the studied area based on the stream sediment and lithogeochemical samples.

As mentioned earlier, the factor analysis was used to reduce the data dimensions and classify them into specific groups. For this purpose, first, the Ln function was used to homogenize the data, and then the FA method was applied. Based on the rotated component matrix (Table 3), 7 different groups were identified. The first group included the Fe, Al, Ca, Mg, Na, Co, and Cu elements, probably related to the host rock and fourth group with Pb, Zn, Mn, and Ag based on the geological evidence of the studied area related to mineralization [1], [43], [93].

After recognition of the elements with most similar behaviors, the whole area was estimated for Pb, Zn, and Cu based on the stream sediment and lithological data. In order to train the LOLIMOT system, the stream sediment data was used as the input (the elements in the mentioned factors) and the lithogeochemical data (Pb, Zn, and Cu) as the output. In the Mial area, the sampling network is irregular for both the stream sediment and lithogeochemical samples, so finding the equivalent samples is very important.

Fishnet in ArcGIS was generated, and the pairs in the same net with the lowest distance were selected according to the assign stream sediment input data to their suitable lithological output data, as they were not exactly from the same coordinate. In this work, 800 m × 600 m cells were applied to assign the input and output data. Moreover, totally 32 data was selected, 70% of the selected data was allocated for training, and the rest for test. For Cu estimation, Fe, Al, Ca, Mg, Na, Co, and Cu in the stream sediment were used as the inputs, and the output was the Cu grade in the lithological data. Furthermore, Pb, Zn, Ag, and Cs from the stream sediment data were inputs, and the outputs were Pb and Zn from the lithological data, respectively. Then these three separate groups of data were used to train the LOLIMOT network. There was only one output, and the neuro-fuzzy network was trained.

The correlation coefficient and accuracy coefficient for the train and test data are shown in Table 5 and Figure 6. The results obtained were acceptable, and the LOLIMOT network was proper for the training process.

Table 5. Correlation coefficient and accuracy coefficient for the train and test data.

Element	Correlation coefficient (%)	Accuracy coefficient (%)-R-Squared value
Pb	97	86
Zn	99	91
Cu	96	84

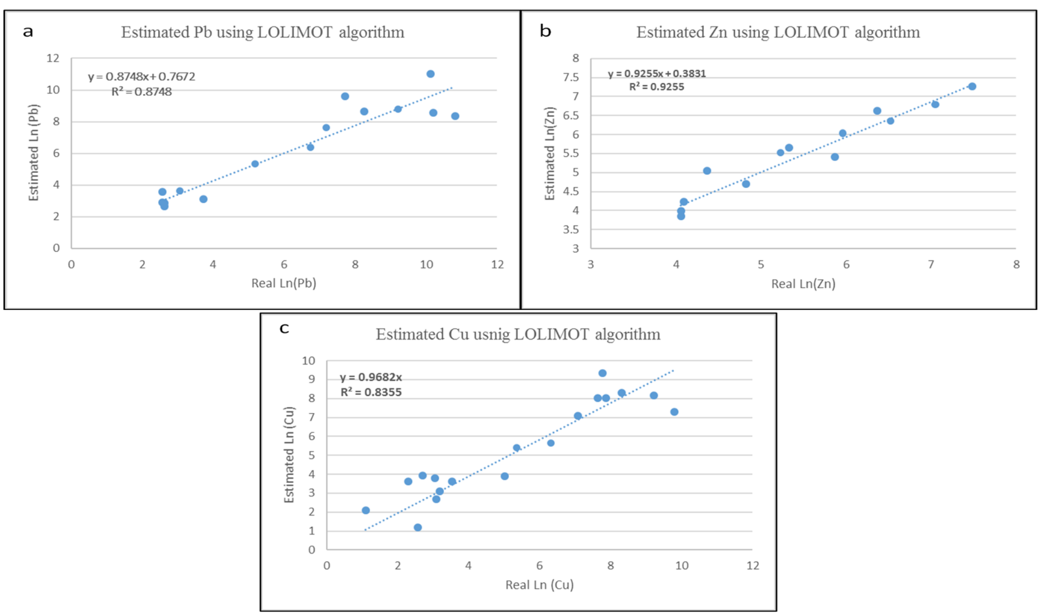

Figure 6. Estimated a) Pb, b) Zn, and c) Cu from the train and test steps using the LOLIMOT algorithm.

In order to evaluate the LOLIMOT operation, the heavy mineral data was applied to validate the predicted anomalies. The results obtained by integration of the estimated Pb, Zn, and Cu grades and the heavy mineral data for each element, respectively, are shown in Figures. 8 to 10. Due to the achieved results, there are two main groups of mineralization, one is in the lapilli tuff and andesitic breccia rock in the SW part of the Mial area and the other one is in the intercalation of red marl and sandy limestone in the Eastern part of the area.

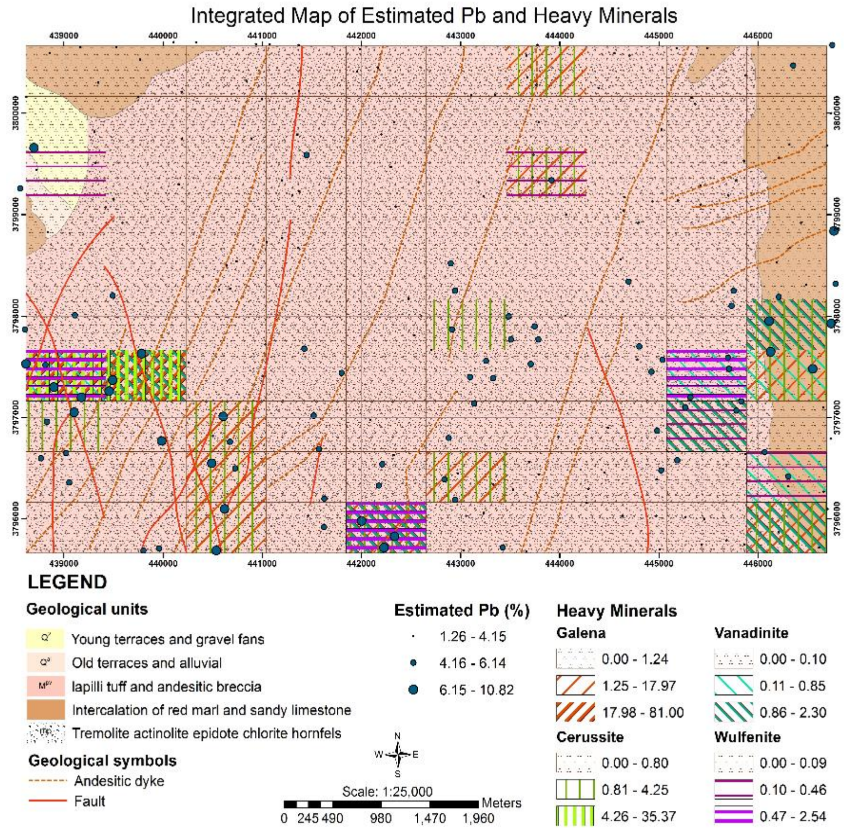

Figure 7. Heavy mineral anomaly map integrated with Pb estimated by LOLIMOT.

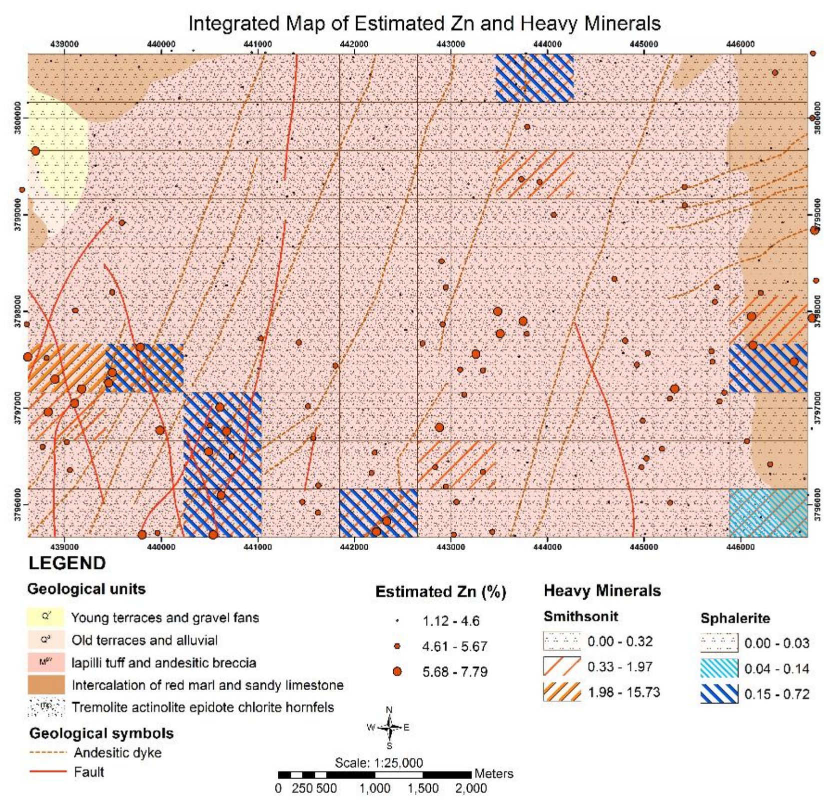

Figure 8. Heavy mineral anomaly map integrated with Zn estimated by LOLIMOT.

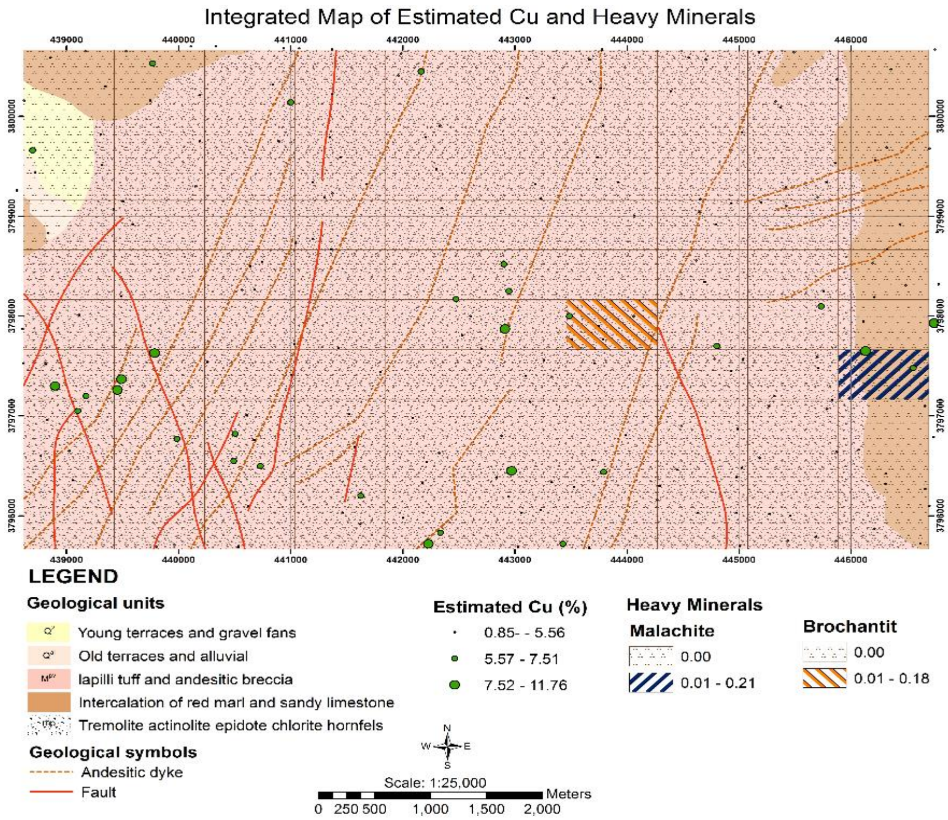

Figure 9. Heavy mineral anomaly map integrated with Cu estimated by LOLIMOT.

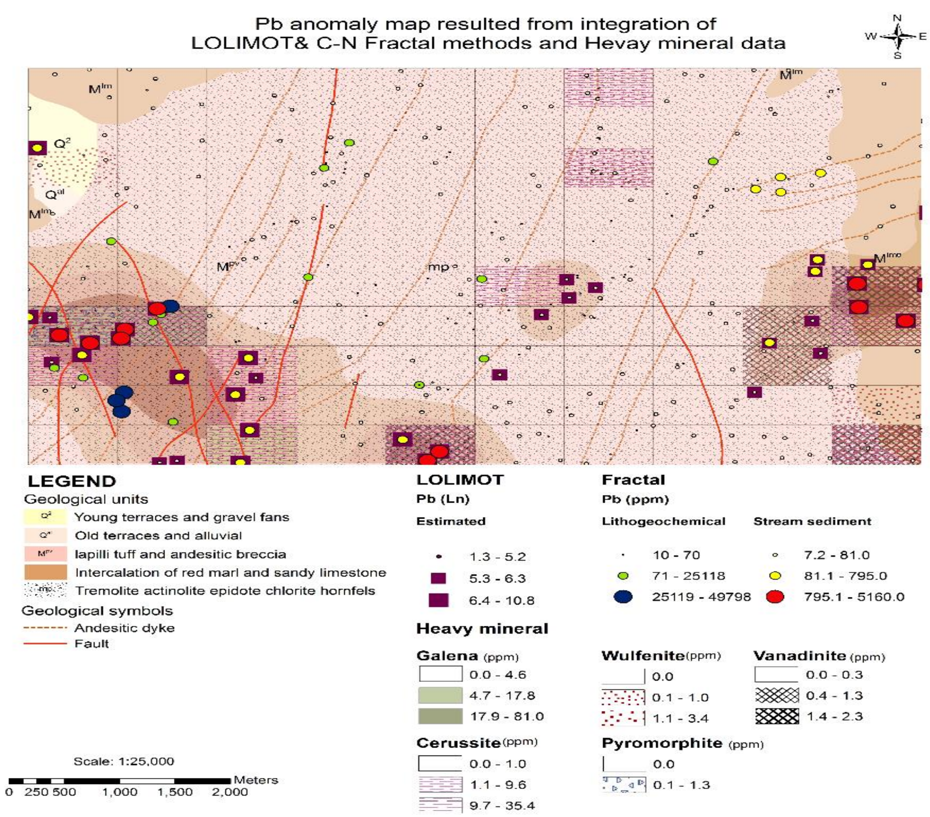

Figure 10. Pb anomaly map resulting from integration of the LOLIMOT and C-N fractal methods with heavy mineral data.

In the SW part of the area, the Pb-Zn and Cu anomalies mostly occurred near an andesitic dike and lineaments, which can show the relation between the mineralization and the structural feature. The mineralization in the Eastern part of the area is mostly related to the Pb and Zn grade and, in a less degree, to Cu anomalies located in the limestone rock. The source of the mineralization based on evidences was not clear but it could be related to Skarn-type of the deposit. The results derived from the LOLIMOT algorithm and the fractal model were integrated to show the most potentialed area for the Pb-Zn and Cu mineralizations in the SW, SE, and central parts of the studied area (Figures. 10-12).

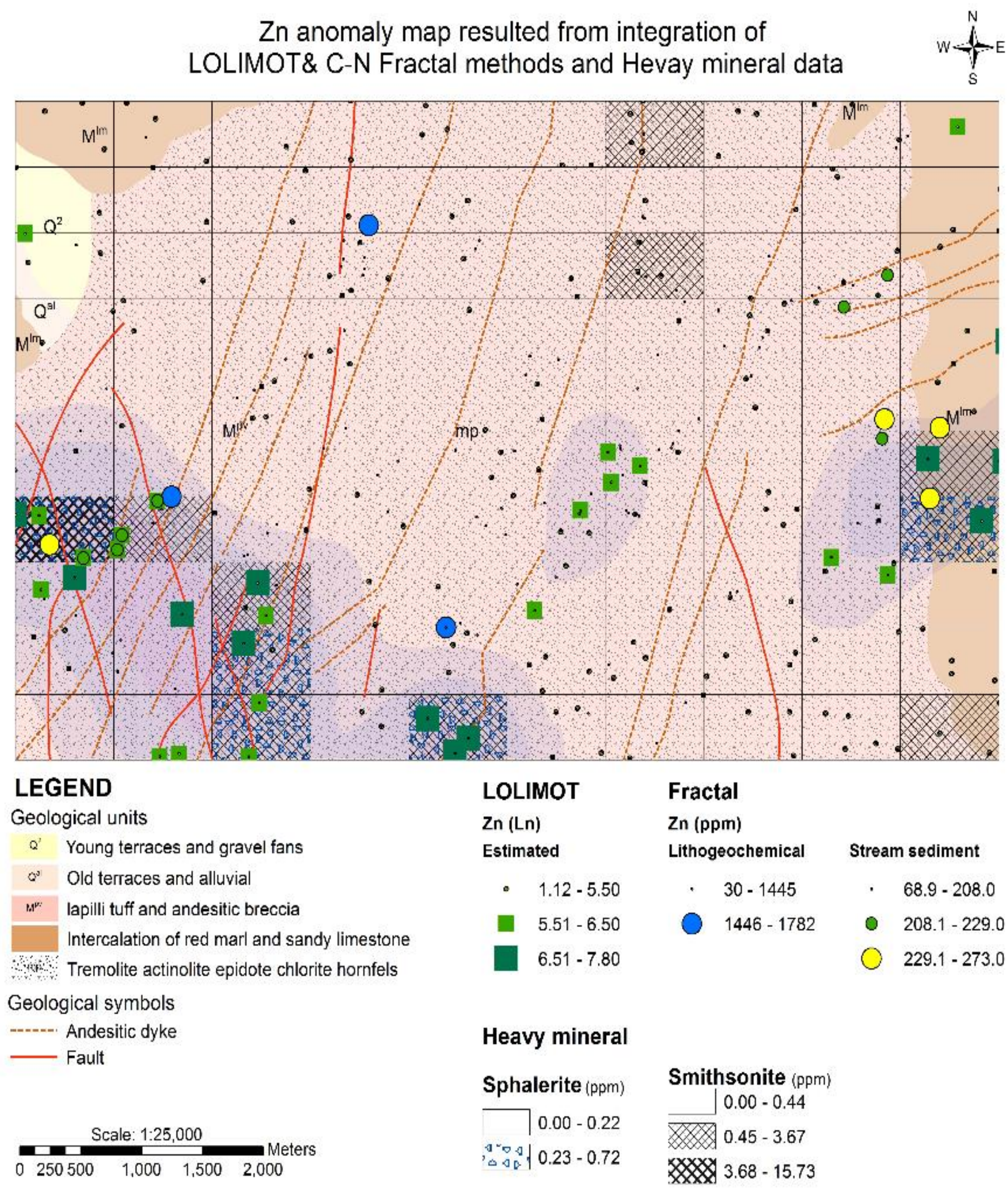

Figure 11. Zn anomaly map resulting from integration of the LOLIMOT and C-N fractal methods with heavy mineral data.

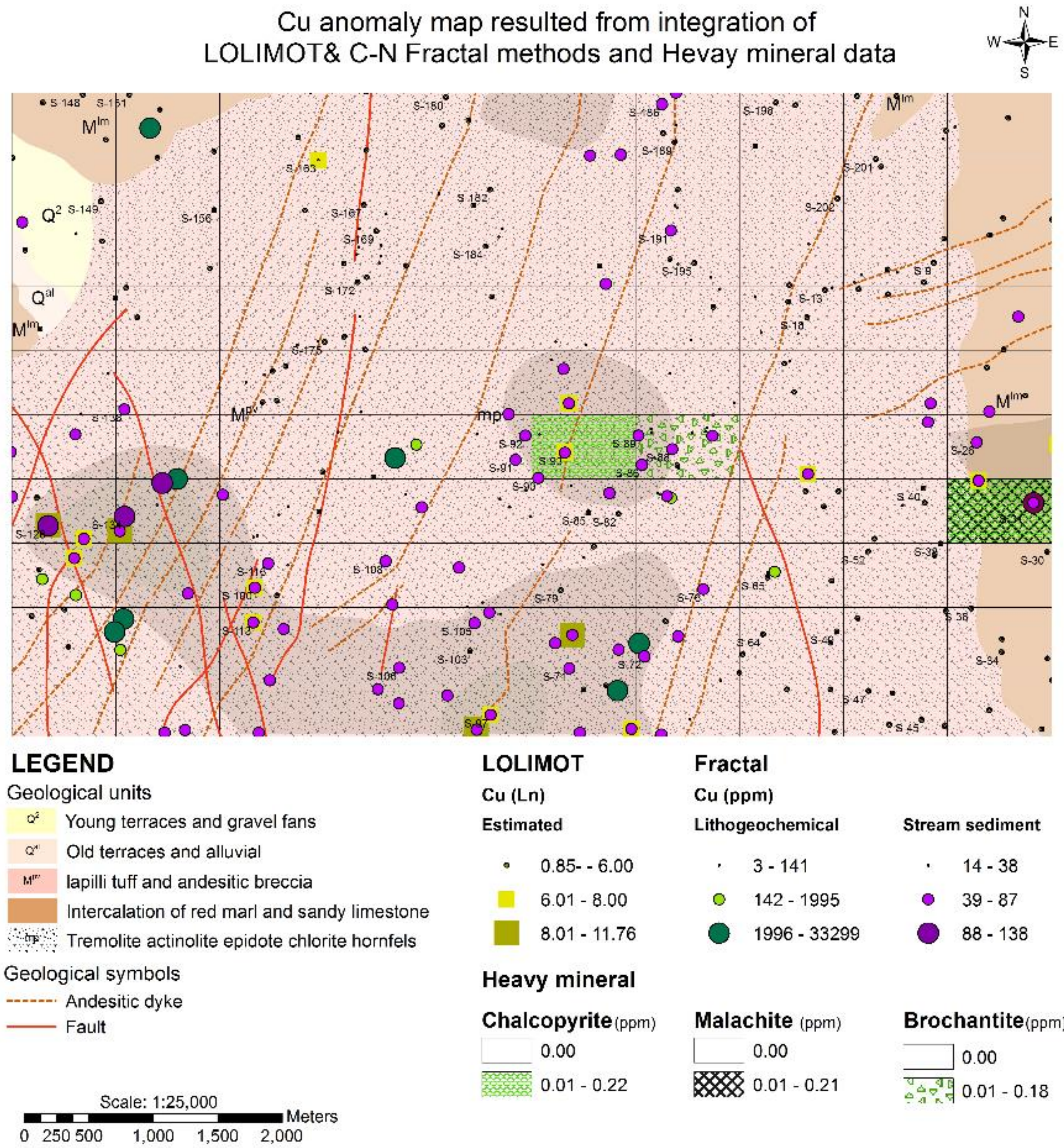

Figure 12. Cu anomaly map resulting from integration of the LOLIMOT and C-N fractal methods with heavy mineral data.

5. Conclusions

In this work, the FA, C-N, and LOLIMOT models were implemented to detect the geochemical anomalies associated with Pb, Zn, and Cu mineralization. The consequences of this work lead to the following conclusions:

1) The hybrid methodology integrating the FA and C-N multi-fractal modeling is a valuable approach for recognizing geochemical anomalies. FA for the stream sediment and lithogeochemical data was applied to combine the multi-element concentration values, whereas F1 and F4 could describe the main Pb, Zn, and Cu mineralization processes successfully in this region. The C-N fractal model was utilized to decompose the mixed Pb, Zn, and Cu geochemical pattern in a complex

geological and structural setting. The results obtained suggest that places with the most fault accumulation and conjugation are highly potentiated areas for mineralization. Also the contact of igneous and sedimentary rocks is another important factor for mineralization occurrence.

2) The neuro-fuzzy LOLIMOT approach was successfully used to establish the accurate geochemical characterization in the Pb, Zn, and Cu anomalies. In order to achieve reliable predictive models, and choose the elements with the most similar behaviors, the FA results were used. The elements in F1 and F4 were applied as the input data to estimate the Cu and Pb-Zn potentials as the output, respectively. The results of this work show that the NFLLM algorithm can be a suitable tool for examining the relationships between the different datasets and geochemical variables to identify the mineral anomalies.
3) The hybrid methodology combining the FA, C-N, and LOLIMOT methods engaged in this work can be used not only to use fine geochemical anomalies where probable mineral resources are presented but also to further improve the factors that control the mineralization and their associated geochemical anomalies.

References

[1]. Agard, P., Omrani, J., Jolivet, L. and Mouthereau, F. (2005). "Convergence history across Zagros (Iran): Constraints from collisional and earlier deformation," Int. J. Earth Sci., vol. 94, no. 3, pp. 401–419.

[2]. Alavi, M. (1994). "Tectonics of the zagros orogenic belt of iran: new data and interpretations," Tectonophysics, vol. 229, no. 3–4, pp. 211–238.

[3]. Berberian, M. (1981). "Zagros, Hindu Kush, Himalaya: Geodynamic Evolution," Geodyn. Ser., vol. 3, pp. 33–69.

[4]. Afzal, P. and Noori, R. (2013). "Reconnassance of Coper and Gold mineralization using analytical hierarchy process (AHP)" J. Min. Metall. Sect. B Metall., no. February 2014, p. 12.

[5]. Liu, Y., Zhou, K. and Cheng, Q. (2017). "A new method for geochemical anomaly separation based on the distribution patterns of singularity indices," Comput. Geosci., vol. 105, no. January. pp. 139–147.

[6]. Daya, A.A. (2012). "Reserve estimation of central part of Choghart north anomaly iron ore deposit through ordinary kriging method." Int. J. Min. Sci. Technol., vol. 22, no. 4, pp. 573–577.

[7]. Zuo, R. and Wang, J. (2016). "Fractal/multifractal modeling of geochemical data: A review," J. Geochemical Explor., vol. 164, pp. 33–41.

[8]. Zhao, J., Chen, S. and Zuo, R. (2016). "Identifying geochemical anomalies associated with Au–Cu mineralization using multifractal and artificial neural network models in the Ningqiang district, Shaanxi, China," J. Geochemical Explor., vol. 164, pp. 54–64.

[9]. Afzal, P., Ahmadi, K. and Rahbar, K. (2017). "Application of fractal-wavelet analysis for separation of geochemical anomalies," J. African Earth Sci., vol. 128, pp. 27–36.

[10]. Nazarpour, A., Paydar, G.R. and Carranza, E. J. M. (2016). "Stepwise regression for recognition of geochemical anomalies: Case study in Takab area, NW Iran," J. Geochemical Explor., vol. 168, pp. 150–162.

[11]. Potra, A., Dodd, J.W. and Ruhl, L.S. (2017). "Distribution of trace elements and Pb isotopes in stream sediments of the Tri-State mining district (Oklahoma, Kansas, and Missouri), USA," Appl. Geochemistry, vol. 82, pp. 25–37.

[12]. Marra, K.R., Elwood Madden, M.E., Soreghan, G.S. and Hall, B.L. (2017)."Chemical weathering trends in fine-grained ephemeral stream sediments of the McMurdo Dry Valleys, Antarctica," Geomorphology, vol. 281, pp. 13–30.

[13]. Zuluaga, M.C., Norini, G., Lima, A., Albanese, S., David, C.P. and De Vivo, B. (2017)."Stream sediment geochemical mapping of the Mount Pinatubo-Dizon Mine area, the Philippines: Implications for mineral exploration and environmental risk," J. Geochemical Explor., vol. 175, pp. 18–35.

[14]. C. Reimann, P. Filzmoser, and R. G. Garrett, "Background and threshold: Critical comparison of methods of determination," Sci. Total Environ., vol. 346, no. 1–3, pp. 1–16, 2005.

[15]. Carranza, E.J.M. (2009). "Controls on mineral deposit occurrence inferred from analysis of their spatial pattern and spatial association with geological features," Ore Geol. Rev., vol. 35, no. 3–4, pp. 383–400.

[16]. Hawkes, B.H.E., Webb, J.S. and Rose, A.W. (1962). "Geochemistry in Mineral Exploration. New York". Harper & Row, New York.

[17]. Herbert Edwin Hawkes, J.S.W. (1972). Geochemistry in Mineral Exploration, 2nd edn. New York: Academic Press.

[18]. Davis, J.C. (2002). "Statistics and data analysis in geology," in Statistics and Data Analysis in Geology. pp. 238–244.

[19]. Afzal, P., Alghalandis, Y.F., Moarefvand, P., Rashidnejad Omran, N. and Asadi Haroni, H. (2012). "Application of power-spectrum-volume fractal method for detecting hypogene, supergene enrichment, leached and barren zones in Kahang Cu porphyry deposit,

Central Iran," J. Geochemical Explor., vol. 112, pp. 131–138.

[20]. M. Eskandarnejad Tehrani, P. Afzal, M. Ghaderi, and M. R. Hosseini, "Delineation of supergene enrichment , hypogene and oxidation zones utilizing staged factor analysis and fractal modeling in Takht- e-Gonbad porphyry deposit , SE Iran," J. Geochemical Explor., vol. 161, pp. 119–127, 2016.

[21]. R. Zuo, "Identifying geochemical anomalies associated with Cu and Pb – Zn skarn mineralization using principal component analysis and spectrum – area fractal modeling in the Gangdese Belt , Tibet (China)," J. Geochemical Explor., vol. 111, no. 1–2, pp. 13–22, 2011.

[22]. M. Jébrak, "Innovations in mineral exploration : Targets , methods and organization since the first globalization period," Université du Québec à Montréal, 2012.

[23]. R. Zuo, "Exploring the effects of cell size in geochemical mapping," J. Geochemical Explor., vol. 112, pp. 357–367, 2012.

[24]. T. Takagi and M. Sugeno, "Fuzzy identification of systems and its applications to modeling and control," IEEE Trans. Syst. Man. Cybern., vol. SMC-15, no. 1, pp. 116–132, Jan. 1985.

[25]. J. Vieira, F. Dias, and A. Mota, "Neuro-fuzzy systems: a survey," in 5th WSEAS NNA International Conference, 2004, pp. 1–6.

[26]. C. Cranganu, H. Luchian, and M. E. Breaban, Artificial Intelligent Approaches in Petroleum Geosciences. Cham: Springer International Publishing, 2015.

[27]. M. . Gardner and S. . Dorling, "Artificial neural networks (the multilayer perceptron)—a review of applications in the atmospheric sciences," Atmos. Environ., vol. 32, no. 14–15, pp. 2627–2636, 1998.

[28]. S. Esmaeilzadeh, A. Afshari, and R. Motafakkerfard, "Integrating Artificial Neural Networks Technique and Geostatistical Approaches for 3D Geological Reservoir Porosity Modeling with an Example from One of Iran's Oil Fields," Pet. Sci. Technol., vol. 31, no. 11, pp. 1175–1187, Jun. 2013.

[29]. L. a. Zadeh, "Fuzzy sets," Inf. Control, vol. 8, no. 3, pp. 338–353, 1965.

[30]. A. B. Jalloh, S. Kyuro, Y. Jalloh, and A. K. Barrie, "Integrating artificial neural networks and geostatistics for optimum 3D geological block modeling in mineral reserve estimation: A case study," Int. J. Min. Sci. Technol., vol. 26, no. 4, pp. 581–585, 2016.

[31]. R. Karami and P. Afzal, "Estimation of Elemental Distributions by Combining Artificial Neural Network and Inverse Distance Weighted (IDW) Based on Lithogeochemical Data in Kahang Porphry Deposit , Central Iran," IFAC Proc. Vol., no. 2, pp. 59–65, 2015.

[32]. S. J. Lee, M.-H. Ahn, and Y. Lee, "APPLICATION OF ARTIFICIAL NEURAL NETWORK FOR THE DIRECT ESTIMATION OF ATMOSPHERIC INSTABILITY FROM A GEOSTATIONARY SATELLITE IMAGER," in Proceedings of the 19th ITSC, 2016, p. 10.

[33]. Q. Cheng, F. P. Agterberg, and S. B. Ballantyne, "The separation of geochemical anomalies from background by fractal methods," J. Geochemical Explor., vol. 51, no. 2, pp. 109–130, Jul. 1994.

[34]. Q. Cheng, F. P. Agterberg, and G. F. Bonham-Carter, "Fractal pattern integration for mineral potential estimation," Nonrenewable Resour., vol. 5, no. 2, pp. 117–130, 1996.

[35]. Q. Cheng and F. P. Agterberg, "Muitifractal Modeling and Spatial Statistics," Math. Geol., vol. 28, no. I, pp. 1–16, 1996.

[36]. Q. Cheng, Y. Xu, and E. Grunsky, "Integrated spatial and spectrum method for geochemical anomaly separation," Nat. Resour. Res., vol. 9, no. 1, pp. 43–52, 2000.

[37]. C. Li, T. Ma., and J. Shi, "Application of a fractal method relating concentrations and distances for separation of geochemical anomalies from background," J. Geochemical Explor., vol. 77, no. 2–3, pp. 167–175, 2003.

[38]. Q. Wang, J. Deng, H. Liu, L. Yang, L. Wan, and R. Zhang, "Fractal models for ore reserve estimation," Ore Geol. Rev., vol. 37, no. 1, pp. 2–14, 2010.

[39]. S. Rezaei, M. Lotfi, P. Afzal, M. R. Jafari, and M. Shamseddin Meigoony, "Delineation of Cu prospects utilizing multifractal modeling and stepwise factor analysis in Noubaran 1:100,000 sheet, Center of Iran," Arab. J. Geosci., vol. 8, no. 9, pp. 7343–7357, 2015.

[40]. G. Chen and Q. Cheng, "Fractal density modeling of crustal heterogeneity from the KTB deep hole," J. Geophys. Res. Solid Earth, vol. 122, no. 3, pp. 1919–1933, 2017.

[41]. F. P. Agterberg, "Multifractal modeling of the sized and grades of giant and supergiant deposits," Int. Geol. Rev., vol. 37, no. 2, pp. 1–8, 1995.

[42]. S. Hassanpour and P. Afzal, "Application of concentration-number (C-N) multifractal modeling for geochemical anomaly separation in Haftcheshmeh porphyry system, NW Iran," Arab. J. Geosci., vol. 6, no. 3, pp. 957–970, 2013.

[43]. P. Afzal, A. Khakzad, P. Moarefvand, N. Rashidnejad Omran, B. Esfandiari, and Y. Fadakar Alghalandis, "Geochemical anomaly separation by multifractal modeling in Kahang (Gor Gor) porphyry system, Central Iran," J. Geochemical Explor., vol. 104, no. 1–2, pp. 34–46, Jan. 2010.

[44]. Q. Cheng, "Singularity theory and methods for mapping geochemical anomalies caused by buried

sources and for predicting undiscovered mineral deposits in covered areas," J. Geochemical Explor., vol. 122, pp. 55–70, 2012.

[45]. L. Daneshvar Saein, I. Rasa, N. Rashidnejad Omran, P. Moarefvand, P. Afzal, and B. Sadeghi, "Application of Number-Size (N-S) Fractal Model to Quantify of the Vertical Distributions of Cu and Mo in Nowchun Porphyry Deposit (Kerman, Se Iran)/Zastosowanie modelu fraktalnego ns (liczba-rozmiar) do ilościowego określenia pionowego rozkładu Cu i Mo w," Arch. Min. Sci., vol. 58, no. 1, pp. 89–105, 2013.

[46]. B. Habing, "Exploratory factor analysis," 2003.

[47]. P. Filzmoser, K. Hron, C. Reimann, and R. Garrett, "Robust factor analysis for compositional data," Comput. Geosci., vol. 35, no. 9, pp. 1854–1861, 2009.

[48]. M. Yousefi, E. J. M. Carranza, and A. Kamkar-Rouhani, "Weighted drainage catchment basin mapping of geochemical anomalies using stream sediment data for mineral potential modeling," J. Geochemical Explor., vol. 128, pp. 88–96, May 2013.

[49]. A. M. Farrell and J. Rudd, "Factor Analysis and Discriminant Validity: A Brief Review of Some Practical Issues," Anzmac, pp. 1–9, 2009.

[50]. J. F. Hair, W. C. Black, B. J. Babin, and R. E. Anderson, Multivariate Data Analysis A Global Perspective, vol. 7. Upper Saddle River NJ: Pearson., 2010.

[51]. M. Yousefi, A. Kamkar-Rouhani, and E. J. M. Carranza, "Geochemical mineralization probability index (GMPI): A new approach to generate enhanced stream sediment geochemical evidential map for increasing probability of success in mineral potential mapping," J. Geochemical Explor., vol. 115, pp. 24–35, 2012.

[52]. B. B. Mandelbrot, The Fractal Geometry of Nature, vol. 8, no. 4. San Francisco: John Wiley & Sons, Ltd, 1983.

[53]. P. Afzal et al., "Delineation of geochemical anomalies based on stream sediment data utilizing fractal modeling and staged factor analysis," J. African Earth Sci., vol. 119, pp. 139–149, Jul. 2016.

[54]. A. Le Méhauté, M. Gerspacher, C. Tricot, M. Gerspacher, and C. Tricot, "Fractal Geometry," in Carbon Black, Routledge, 2018, pp. 245–270.

[55]. M. A. Gonçalves, "Characterization of Geochemical Distributions Using Multifractal Models," Math. Geol., vol. 33, no. 1, pp. 41–61, 2001.

[56]. E. J. M. Carranza, "FRACTAL ANALYSIS OF GEOCHEMICAL ANOMALIES," in Geochemical Anomaly and Mineral Prospectivity Mapping in GIS, vol. 11, E. M. Hale, Ed. Enschede, The Netherlands: Elsevier B.V., 2009, pp. 85–114.

[57]. J. Deng, Q. Wang, L. Yang, Y. Wang, Q. Gong, and H. Liu, "Delineation and explanation of geochemical anomalies using fractal models in the Heqing area, Yunnan Province, China," J. Geochemical Explor., vol. 105, no. 3, pp. 95–105, Jun. 2010.

[58]. P. Afzal, "Classification of Coking Coals in C1 Seam of East-Parvadeh Coal Deposit , Central Iran Using Multifractal Modeling," Iran. J. Earth Sci., vol. 6, pp. 108–113, 2014.

[59]. H. Du and N. Zhang, "Application of evolving Takagi-Sugeno fuzzy model to nonlinear system identification," Appl. Soft Comput., vol. 8, no. 1, pp. 676–686, Jan. 2008.

[60]. A. Jimenez, B. M. Al Hadithi, and F. Matia, "Extended Matrix Approach for the Identification of Takagi-Sugeno Fuzzy Model," IFAC Proc. Vol., vol. 42, no. 19, pp. 13–19, 2009.

[61]. N. Allahverdi, A. Tunali, H. Işik, and H. Kahramanli, "A Takagi–Sugeno type neuro-fuzzy network for determining child anemia," Expert Syst. Appl., vol. 38, no. 6, pp. 7415–7418, Jun. 2011.

[62]. N. Kumaresan and K. Ratnavelu, "Optimal control for stochastic linear quadratic singular neuro Takagi-Sugeno fuzzy system with singular cost using genetic programming," Appl. Soft Comput., vol. 24, pp. 1136–1144, Nov. 2014.

[63]. S. Rastegar, R. Araújo, and J. Mendes, "Online identification of Takagi–Sugeno fuzzy models based on self-adaptive hierarchical particle swarm optimization algorithm," Appl. Math. Model., vol. 45, pp. 606–620, 2017.

[64]. Y. Liu and D. Yang, "Convergence analysis of the batch gradient-based neuro-fuzzy learning algorithm with smoothing L1/2 regularization for the first-order Takagi–Sugeno system," Fuzzy Sets Syst., vol. 319, pp. 28–49, 2017.

[65]. O. Nelles, "Local Linear Model Trees for On-Line Identification of Time-Variant Nonlinear Dynamic Systems," Artif. Neural Networks—ICANN 96, pp. 115–120, 1996.

[66]. O. Nelles, Nonlinear system identification: from classical approaches to neural networks and fuzzy models. Springer Science & Business Media, 2001.

[67]. C. Lucas, R. M. Milasi, and B. N. Araabi, "Intelligent Modeling and Control of Washing Machine Using Locally Linear Neuro-Fuzzy (Llnf) Modeling and Modified Brain Emotional Learning Based Intelligent Controller (Belbic)," Asian J. Control, vol. 8, no. 4, pp. 393–400, 2008.

[68]. J. D. Martínez-Morales, E. Palacios, and G. A. V. Carrillo, "Modeling of internal combustion engine emissions by LOLIMOT algorithm," Procedia Technol., vol. 3, pp. 251–258, 2012.

[69]. B. Yi, J. Ferdinand, N. Simm, and F. Bonarens, "Application of Local Linear Steering Models with

Model Predictive Control for Collision Avoidance Maneuvers," IFAC-PapersOnLine, vol. 49, no. 15, pp. 187–192, 2016.

[70]. A. Pedram, M. Jamali, and T. Pedram, "Local linear model tree (LOLIMOT) reconfigurable parallel hardware," Trans. Eng. Comput. Technol., vol. 13, no. May, pp. 96–101, 2006.

[71]. T. Münker and O. Nelles, "Nonlinear System Identification with Regularized Local FIR Model Networks," IFAC-PapersOnLine, vol. 49, no. 5, pp. 61–66, 2016.

[72]. J. Rehrl, D. Schwingshackl, and M. Horn, A modeling approach for HVAC systems based on the LoLiMoT algorithm, vol. 19, no. 3. IFAC, 2014.

[73]. Collette Yann and Gougeon Samuel, "ATOMS : Lolimot details," Modeling - Control Tools Data Analysis - Statistics - Neural networks, 2018. [Online]. Available: https://atoms.scilab.org/toolboxes/lolimot. [Accessed: 10-Dec-2018].

[74]. O. Nelles, O. Hecker, and R. Isermann, "Automatic model selection in local linear model tree (LOLIMOT) for nonlinear system identification of a transport delay process," 11th IFAC Symp. Syst. Identif., vol. 30, no. 11, pp. 699–704, 1997.

[75]. D. Schwingshackl, J. Rehrl, M. Horn, J. Belz, and O. Nelles, "Model extension for model based MIMO control in HVAC systems," J. Build. Eng., vol. 11, pp. 224–229, 2017.

[76]. R. Zimmerschied and R. Isermann, "Nonlinear System Identification of Block-oriented Systems using Local Affine Models," IFAC Proc. Vol., vol. 42, no. 10, pp. 658–663, 2009.

[77]. R. Razavi-Far, H. Davilu, V. Palade, and C. Lucas, "NEURO-FUZZY BASED FAULT DIAGNOSIS OF A STEAM GENERATOR," IFAC Proc. Vol., vol. 42, no. 8, pp. 1180–1185, 2009.

[78]. Dong, Q., Sun, Y. and Li, P. (2017). A novel forecasting model based on a hybrid processing strategy and an optimized local linear fuzzy neural network to make wind power forecasting: A case study of wind farms in China. Renewable Energy, 102, 241-257.

[79]. Marwaha, M., Valasek, J. and Singla, P. (2009). Nonlinear system identification of discrete systems using GLO-MAP. In AIAA Guidance, Navigation, and Control Conference (p. 5881).

[80]. Schwingshackl, D., Rehrl, J. and Horn, M. (2016). LoLiMoT based MPC for air handling units in HVAC systems. Building and environment. 96: 250-259.

[81]. Gholipour, A., Araabi, B. N. and Lucas, C. (2006). Predicting chaotic time series using neural and neurofuzzy models: a comparative study. neural processing letters. 24 (3): 217-239.

[82]. R. Razavi-Far, H. Davilu, V. Palade, and C. Lucas, "Model-based fault detection and isolation of a steam generator using neuro-fuzzy networks," Neurocomputing, vol. 72, no. 13–15, pp. 2939–2951, Aug. 2009.

[83]. B. Yi, J. Ferdinand, N. Simm, and F. Bonarens, "Application of Local Linear Steering Models with Model Predictive Control for Collision Avoidance Maneuvers," IFAC-PapersOnLine, vol. 49, no. 15, pp. 187–192, 2016.

[84]. O. Nelles, A. Fink, and I. Rolf, "Local Linear Model Trees (LOLIMOT) Toolbox for Nonlinear System Identification Axes-Oblique Partitioning Strategies for Local Model Networks," IFAC Proc. Vol., vol. 33, no. 15, pp. 845–850, 2000.

[85]. T. Münker and O. Nelles, "Nonlinear System Identification with Regularized Local FIR Model Networks," in IFAC-PapersOnLine, 2016, vol. 49, no. 5, pp. 61–66.

[86]. P. Agard et al., "Zagros orogeny: a subduction-dominated process," Geol. Mag. Cambridge Univ. Press, vol. 148, no. 5–6, pp. 692–725, 2011.

[87]. F. Rashidinejad, M. Osanloo, and B. Rezai, "Cut of Grades Optimization with Environmental management; a case study: Sungun Copper Porphyry Project," IUST Int. J. Eng. Sci., vol. 19, no. 5–1, pp. 1–13, 2009.

[88]. F. Ayati, F. Yavuz, H. H. Asadi, J. P. Richards, and F. Jourdan, "Petrology and geochemistry of calc-alkaline volcanic and subvolcanic rocks, Dalli porphyry copper–gold deposit, Markazi Province, Iran," Int. Geol. Rev., vol. 55, no. 2, pp. 1–27, 2013.

[89]. M. Rezaei-Kahkhaei, C. Galindo, R. J. Pankhurst, and D. Esmaeily, "Magmatic differentiation in the calc-alkaline Khalkhab-Neshveh pluton, Central Iran," J. Asian Earth Sci., vol. 42, no. 3, pp. 499–514, 2011.

[90]. Zarasvandi, A., Rezaei, M., Sadeghi, M., Lentz, D., Adelpour, M. and Pourkaseb, H. (2015). Rare earth element signatures of economic and sub-economic porphyry copper systems in Urumieh–Dokhtar Magmatic Arc (UDMA), Iran. Ore geology reviews. 70: 407-423.

[91]. Asadi, H. H., Porwal, A., Fatehi, M., Kianpouryan, S. and Lu, Y.J. (2015). Exploration feature selection applied to hybrid data integration modeling: Targeting copper-gold potential in central Iran. Ore Geology Reviews. 71: 819-838.

[92]. Aliyari, F., Rastad, E. and Mohajjel, M. (2012). Gold Deposits in the Sanandaj–Sirjan Zone: Orogenic Gold Deposits or Intrusion-Related Gold Systems?. Resource Geology. 62 (3): 296-315.

[93]. Aghazadeh, M., Hou, Z., Badrzadeh, Z. and Zhou, L. (2015). Temporal–spatial distribution and tectonic setting of porphyry copper deposits in Iran: constraints from zircon U–Pb and molybdenite Re–Os geochronology. Ore geology reviews. 70, 385-406..

[94]. Zarasvandi, A., Rezaei, M., Raith, J., Lentz, D., Azimzadeh, A.M. and Pourkaseb, H. (2015). “Geochemistry and fluid characteristics of the Dalli porphyry Cu–Au deposit, Central Iran,” J. Asian Earth Sci., vol. 111, pp. 175–191.

[95]. Hosseini, M.R. Hassanzadeh, J., Alirezaei, S., Sun, W. and Li, C.Y. (2017). “Age revision of the Neotethyan arc migration into the southeast Urumieh-Dokhtar belt of Iran: Geochemistry and U–Pb zircon geochronology,” Lithos, vol. 284, pp. 296–309.

[96]. Fazeli, B., Khalili, M., Toksoy Köksal, F., Esfahani, M.M. and Beavers, R. (2017).“Petrological constraints on the origin of the plutonic massif of the Ghaleh Yaghmesh area, Urumieh–Dokhtar magmatic arc, Iran,” J. African Earth Sci., vol. 129, pp. 233–247.

[97]. Aitchison, J. (1982). “The Statistical Analysis of Compositional Data,” J. R. Stat. Soc. Ser. B. Methodol., vol. 44, no. 2, pp. 139–177.

[98]. Rantitsch, G. (2000) .“Application of fuzzy clusters to quantify lithological background concentrations in stream-sediment geochemistry,” J. Geochemical Explor., vol. 71, no. 1, pp. 73–82.

[99]. Gao, C., Bao, K., Lin, Q., Zhao, H., Zhang, Z., Xing, W. and Wang, G. (2014). Characterizing trace and major elemental distribution in late Holocene in Sanjiang Plain, Northeast China: Paleoenvironmental implications. Quaternary international. 349: 376-383.

[100]. Almasi, A., Jafarirad, A., Afzal, P., and Rahimi, M. (2015). Prospecting of gold mineralization in Saqez area (NW Iran) using geochemical, geophysical and geological studies based on multifractal modelling and principal component analysis. Arabian Journal of Geosciences. 8 (8): 5935-5947.

[101]. Parsa, M., Maghsoudi, A., Carranza, E. J. M., and Yousefi, M. (2017). Enhancement and mapping of weak multivariate stream sediment geochemical anomalies in Ahar Area, NW Iran. Natural Resources Research. 26 (4): 443-455.

[102]. Muller, J., Kylander, M., Martinez-Cortizas, A., Wüst, R.A., Weiss, D., Blake, K., and Garcia-Sanchez, R. (2008). The use of principle component analyses in characterising trace and major elemental distribution in a 55 kyr peat deposit in tropical Australia: implications to paleoclimate. *Geochimica et Cosmochimica Acta. 72* (2): 449-463.

شناسایی آنومالی‌های ژئوشیمیایی با استفاده از مدلسازی عصبی-فازی لولیموت و فرکتال در منطقه میال، ایران مرکزی

مهرنوش علی‌پور شهسواری[1]، پیمان افضل[2] و امین حکمت‌نژاد[3]

1- دانشکده مهندسی معدن، دانشکده فنی، دانشگاه تهران، تهران، ایران
2- دانشکده مهندسی معدن، شعبه تهران جنوب، دانشگاه آزاد اسلامی، تهران، ایران
3- دانشکده مهندسی معدن، مرکز تکنولوژی معدنکاری پیشرفته، دانشگاه شیلی، شیلی

ارسال 2019/5/26، پذیرش 2019/11/6

* نویسنده مسئول مکاتبات: Mehrnoosh.ap@gmail.com

چکیده:

کمان ماگمایی ارومیه- دختر به عنوان یک کمان کانی‌زایی مهم برای انواع کانی سازی‌های پرفیری، پراکنده، رگه‌ای و پلی‌متال به شمار می‌رود. هدف از انجام این مطالعه شناسایی و تعیین آنومالی‌های ژئوشیمیایی برای اکتشافات سرب، روی و مس در محدوده میال واقع در کمان ماگمایی ارومیه- دختر است. آنالیز فاکتوری، مدل فرکتالی عیار- تعداد و الگوریتم درخت مدل خطی محلی (لولیموت) بدین منظور مورد استفاده قرار گرفته است. آنالیز فاکتوری به منظور شناسایی ارتباط بین عناصر و دسته‌بندی آن‌ها به کار گرفته شد. داده‌های دسته‌بندی شده، براساس عناصر مرتبط به منظور آموزش الگوریتم لولیموت به کار گرفته شدند. نتایج بدست آمده از الگوریتم لولیموت نمایانگر وجود آنومالی در مناطقی است که در آن نمونه‌برداری ژئوشیمیایی صورت نگرفته است. علاوه بر این، نمودارهای عیار- تعداد براساس نمونه‌های لیتوژئوشیمیایی و رسوبات آبراهه‌ای، برای عناصر هدف ترسیم شدند که می‌تواند نمایانگر پتانسیل‌های کانی‌زایی از عناصر مطلوب باشند. نتایج بدست آمده از مدل‌سازی‌های لولیموت و فرکتال حاکی از وجود مناطقی در بخش‌های جنوب‌شرقی و شرق منطقه هستند که می‌توانند برای اکتشافات آتی عناصر مس، سرب و روی مورد بررسی قرار بگیرند.

کلمات کلیدی: مدل فرکتالی عیار- تعداد، درخت مدل خطی محلی (لولیموت)، میال.